

Antibody-Drug Conjugates (ADCs): Quantifying the Bystander Effect in Heterogeneous Tumour Microenvironments A Comprehensive Review

Sanjula Gautam¹, Ananya Maurya², Pyare Lal³, Prateek Singh⁴, Adarsh Mishra⁵, and Mamta Tiwari⁶

¹*School of Pharmaceutical Sciences, Chhatrapati Shahu Ji Maharaj University*

Email: gautamsanjula9@gmail.com

²*School of Pharmaceutical Sciences, Chhatrapati Shahu Ji Maharaj University*

Email: ananya224143@gmail.com

³*Lohia Aerospace System - Lohia Group, Kanpur, Uttar Pradesh*

Email: er.pyarel39kcnit@gmail.com

⁴*School of Pharmaceutical Sciences, Chhatrapati Shahu Ji Maharaj University*

Email: prateeksingh34421@gmail.com

⁵*School of Pharmaceutical Sciences, Chhatrapati Shahu Ji Maharaj University*

Email: [iamadarshmishra007@gmail.com](mailto:iamadashmishra007@gmail.com)

⁶*School of Pharmaceutical Sciences, Chhatrapati Shahu Ji Maharaj University*

(Corresponding Author) Email: mamta1712@gmail.com

ORCID: 0009-0001-0534-4772

ABSTRACT

Antibody-drug conjugates (ADCs) are a new paradigm in targeted oncology that marries the specificity of a monoclonal antibody with the potency of a small molecule payload. Many ADCs possess a characteristic property that is important to their therapeutic effects: the bystander effect, which refers to diffusion of a cytotoxic payload from an antigen-positive (Ag⁺) target cell across cell membranes to kill neighboring antigen-negative (Ag⁻) cells in the tumour microenvironment (TME). In heterogeneous solid tumours, where antigens are not always expressed or not expressed in the same pattern throughout the tumour, this phenomenon is particularly important, as without it, the efficacy of ADC would be limited. The mechanisms, determinants, and quantitative aspects of the ADC bystander effect are fully reviewed. We systematically explore how the combined effect of linker chemistry (cleavable versus non-cleavable), payload physicochemical properties (lipophilicity, charge, molecular weight), DAR, receptor expression heterogeneity and TME architecture collectively impact the extent and spatial reach of bystander killing. We also examine cutting-edge experimental models, such as 3D tumour spheroids, co-culture cytotoxicity assays, microfluidic tumour-on-chip platforms, multiplexed spatial imaging and intravital microscopy, as well as mathematical models, from ordinary differential equation (ODE) based PK/PD models to agent-based models and reaction-diffusion partial differential equations (PDEs). To gain insights into the bystander activity of clinically approved ADCs and how this contributes to clinical benefit in antigen-heterogeneous tumours, clinical evidence from approved ADCs such as trastuzumab deruxtecan (T-DXd), sacituzumab govitecan, brentuximab vedotin and polatuzumab vedotin is discussed. Finally, we review the resistance mechanisms, off-target bystander toxicity, rational ADC design to optimise the bystander therapeutic window and future directions such as next generation bispecific ADCs and immunological bystander synergy.

Keywords : Antibody-Drug Conjugate · Bystander Effect · Tumour Microenvironment · Antigen Heterogeneity · Pharmacokinetics/Pharmacodynamics · Drug Delivery · Oncology · Mathematical Modelling · Cleavable Linker · Payload Diffusion.

How to cite this article: Gautam S, Maurya A, Lal P, Singh P, Mishra A, Tiwari M. Antibody-Drug Conjugates (ADCs): Quantifying the Bystander Effect in Heterogeneous Tumour Microenvironments: A Comprehensive Review. *Int J Drug Deliv Technol.* 2026;16(51s): 786-803. DOI: 10.25258/ijddt.16.51s.61

1. INTRODUCTION

The emergence of antibody-drug conjugates has revolutionized the field of cancer drug therapy. Conceived in Paul Ehrlich's vision of a 'magic bullet' that could selectively deliver a cytotoxic agent to a tumour cell, without affecting the surrounding normal cells, ADCs have evolved over 40 years, from experimental constructs to a class of approved medicines for haematological malignancies and solid tumours (Beck et al., 2017). To date, the United States Food and Drug Administration (FDA) has approved over a dozen ADCs, and hundreds of other candidates are in clinical

development. Although they are designed to be targeted, the simple model of ADC killing cells (antigen binding, internalisation, payload delivery, cell death) doesn't account for one of the key additional mechanisms that significantly enhances the therapeutic effects of ADC: the bystander effect. The bystander effect results in diffusion of the released payload through the extracellular space as well as through gap junctions at adjacent cells that are Ag⁻ which results in lethal concentrations of payload (Kovtun et al., 2010; Staudacher & Brown, 2017). This activity is not just an epiphenomenon, but a clinically determinate property that

differentiates between ADCs that are effective against a heterogeneous tumour from those that fail because of the lack of complete antigen coverage. Heterogeneity of tumour antigens exists in all types of tumors. Single cell and spatial transcriptomics analysis regularly shows that even tumours that are classified as 'antigen-positive' have a significant proportion of Ag-low or even Ag-negative cells at baseline, whilst clonal evolution, under selective therapeutic pressure, further diminishes antigen expression (Swaminathan et al., 2023). In the absence of bystander effect these Ag-negative subpopulations would not be eliminated by ADC and would set up recurrence. The bystander effect is difficult to quantify. Not directly measured in standard bulk cytotoxicity assays, it comes about through a combination of various physicochemical and biological parameters and can be very different depending on tumour types, TME composition and ADC designs. Mathematical modelling has become an essential approach for incorporating these parameters into a predictive model that can be used to inform ADC optimisation and clinical trial design (Shah et al., 2012; Thurber et al., 2012). This review systematically and comprehensively examines the molecular mechanisms, quantitative determinants, experimental approaches toward the assessment of the ADC bystander effect, mathematical models used to predict it and clinical evidence and implications regarding resistance and rational drug design. We attempt to gather the vast amount of literature emerging in the field into a conceptual framework that can be used by researchers and clinicians.

2. ADC ARCHITECTURE AND PHARMACOLOGY

2.1 Structural Components

An ADC is comprised of three main elements: a monoclonal antibody (mAb), a warhead, or cytotoxic payload, and a chemical linker that joins the mAb to the warhead (Chari et al., 2014). The antibody is usually of the IgG1 subclass allowing effector functions (ADCC/ADCP) relevant to antitumour immunity and neonatal Fc receptor (FcRn)-mediated recycling resulting in a serum half life of ~21 days. Tumour-restricted or tumour-enriched expression, competence of antigen to be internalised following antibody

binding, and lack of antigen shedding that would sequester the ADC in the circulation are the characteristics that target antigens need to have (Beck et al., 2017). With cell-killing activity in the picomolar to subnanomolar range, payloads are very potent agents, usually 100-fold to 10,000-fold more cytotoxic than conventional chemotherapeutics. There are three major classes of payloads, namely: (1) tubulin polymerisation inhibitors (auristatins: MMAE, MMAF; maytansinoids: DM1, DM4), (2) DNA double-strand break inducers (calicheamicin, duocarmycin, pyrrolobenzodiazepine [PBD] dimers), and (3) topoisomerase I inhibitors (SN-38 in sacituzumab; DXd in trastuzumab deruxtecan) (Doronina et al., 2003; Nakada et al., 2019). The linker is a bifunctional chemical entity, which stabilizes ADC in the systemic circulation and allows efficient release of the payload at the tumour site. The cleavable linkers such as acid-labile hydrazones (takes advantage of the lowered endosomal pH), acid-labile disulfide bonds (which are reduced by the presence of reducing agent glutathione in the cell), and acid-labile protease sensitive peptides (val-cit-pabc is a cathepsin B substrate, and ala-ala-asn is a legumain substrate; Jeffrey et al., 2006) release free, membrane permeable payload upon the internalization and incubation in the lysosomes. Non-cleavable linkers (succinimidyl-4-(N-maleimidomethyl)cyclohexane-1-carboxylate, SMCC) will only release the payload when the antibody is completely catabolized, after which the resulting amino acid-drug adduct is usually charged and membrane-impermeable (Erickson et al., 2006). The number of drug molecules per antibody (drug-antibody ratio or DAR) is a key determinant of both efficacy and tolerability. Conventional stochastic conjugation results in heterogeneous DAR distributions (DAR 0–8) of which the mean is usually approximately 3.5–4. Homogeneous DAR products have improved PK and therapeutic index and can be generated using site-specific conjugation technologies, such as engineered cysteines, unnatural amino acids and enzymatic methods (Deonarain et al., 2015). Next generation ADCs like T-DXd can also be designed to have a high DAR (~8) using stable cleavable linkers without the associated aggregation liability of previous high-DARs.

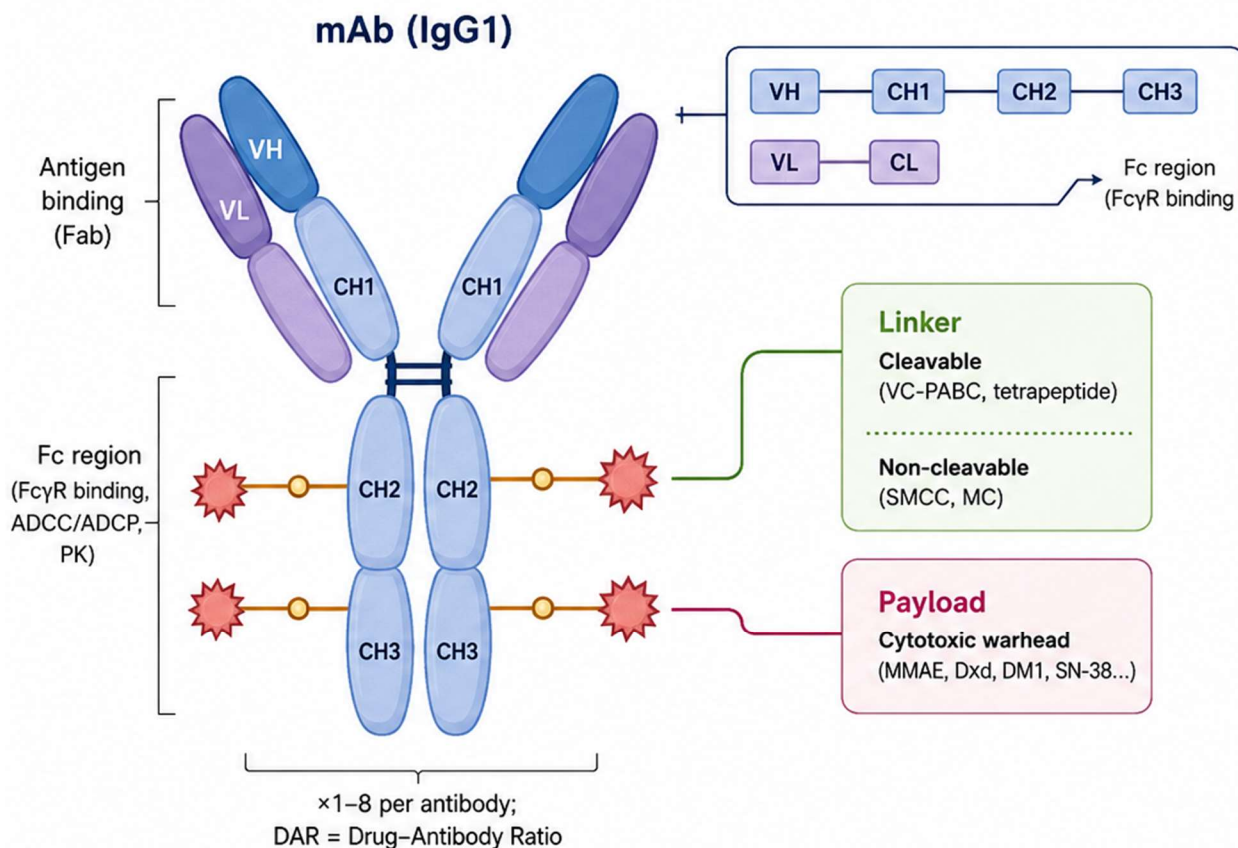


Figure 1. ADC architecture showing the monoclonal antibody, cleavable and non-cleavable linker options, and cytotoxic payload. DAR = drug-antibody ratio; VH = variable heavy chain; VL = variable light chain; Fc = crystallisable fragment.

Table 1. Clinically approved ADCs: molecular targets, linker types, payloads, DAR, and indications.

ADC Name	Target Antigen	Linker Type	Payload	DAR	Indication	FDA Approval Year
Trastuzumab emtansine (T-DM1)	HER2	Non-cleavable (SMCC)	DM1 (maytansinoid)	3.5	HER2+ breast cancer	2013
Brentuximab vedotin	CD30	Cleavable (MC-VC-PABC)	MMAE (auristatin)	4.0	Classical HL, sALCL	2011
Gemtuzumab ozogamicin	CD33	Acid-labile (hydrazone)	Calicheamicin	~2–3	AML	2000/2017

ADC Name	Target Antigen	Linker Type	Payload	DAR	Indication	FDA Approval Year
Inotuzumab ozogamicin	CD22	Acid-labile (hydrazone)	Calicheamicin	~6	ALL	2017
Polatuzumab vedotin	CD79b	Cleavable (MC-VC-PABC)	MMAE (auristatin)	3.5	DLBCL	2019
Trastuzumab deruxtecan (T-DXd)	HER2	Cleavable (tetrapeptide)	DXd (exatecan)	~8	HER2+ breast/gastric/lung	2019
Sacituzumab govitecan	Trop-2	Cleavable (CL2A)	SN-38 (irinotecan)	~7.6	TNBC, UC	2020
Belantamab mafodotin	BCMA	Non-cleavable (MC)	MMAF (auristatin)	3.9	Multiple myeloma	2020
Loncastuximab tesirine	CD19	Cleavable (VC)	SG3199 (PBD dimer)	~2.3	DLBCL	2021
Tisotumab vedotin	TF	Cleavable (MC-VC-PABC)	MMAE (auristatin)	3.9	Cervical cancer	2021
Mirvetuximab soravtansine	FR α	Cleavable (sulfo-SPDB)	DM4 (maytansinoid)	3.5	Ovarian cancer	2022
Datopotamab deruxtecan	Trop-2	Cleavable (tetrapeptide)	DXd (exatecan)	~4	Lung/breast cancer	2024
Ifinatamab deruxtecan	B7-H3	Cleavable (tetrapeptide)	DXd (exatecan)	~8	SCLC	2024

Note. HL = Hodgkin lymphoma; sALCL = systemic anaplastic large cell lymphoma; AML = acute myeloid leukaemia; ALL = acute lymphoblastic leukaemia; DLBCL = diffuse large B-cell lymphoma; TNBC = triple-negative breast cancer; UC = urothelial carcinoma; SCLC = small cell lung cancer; FR α = folate receptor alpha; TF = tissue factor; BCMA = B-cell maturation antigen; DAR = drug-antibody ratio.

2.2 ADC Pharmacokinetics

The PK of ADC PK is regulated by the interplay of antibody PK (long half-life, recycling via FcRn, target-mediated drug disposition [TMDD]) and small-molecule payload PK (short half-life, broad tissue distribution) (Lu et al., 2020). The

ADC can be seen in plasma as three species: intact conjugate, deconjugated antibody (DAR 0), and free payload. Off-target toxicities are caused by deconjugation, either by plasma esterases or by retro-Michael reactions on maleimide linkers or by hydrolysis. The ADC distributes in two phases after IV

administration: a rapid distribution phase and a slower elimination phase with a terminal half-life of 2-7 days for conjugated antibody. The antibody binding site barrier (BSB), vascular permeability, interstitial fluid pressure and diffusion distances in avascular regions of the tumour govern antibody penetration and also influence bystander effect magnitude by controlling the location and concentration of free payload released (Thurber et al., 2012; Khera & Thurber, 2018).

3. MECHANISMS OF THE BYSTANDER EFFECT

3.1 Canonical Pathway: Extracellular Diffusion

The canonical bystander mechanism involves five steps. The first step is for the ADC to bind to its cognate antigen on the surface of an Ag⁺ tumour cell through the variable domain of the antibody portion. The second step involves receptor mediated endocytosis that brings the ADC - antigen complex into an early endosome. Third, progressive acidification of the endosomes and fusion with lysosomes (pH 4.5 - 5.0) leads to linker cleavage (for acid labile or protease sensitive

linkers) or to complete antibody catabolism to release the payload. Finally, the released payload (provided it is lipophilic and membrane permeable) crosses the lysosomal membrane, escapes from the target cell, and reaches the extracellular space. Fifth, the diffusing payload moves into neighbouring Ag⁻ cells down its concentration gradient and causes cell death by its primary mechanism of action (tubulin disruption, DNA damage, or topoisomerase inhibition) (Li et al., 2016). This extracellular diffusion is quantified using the bystander radius (R_b), the distance from the releasing Ag⁺ cell to where the extracellular payload concentration is the same as the cellular IC₅₀. The value of R_b is mainly dictated by three parameters: the diffusion coefficient of the payload in the tumour interstitium (D) which is typically in the range $10^{-7} - 10^{-6}$ cm²/s for small molecules, the extracellular degradation rate constant (k_{deg}) and the intracellular release flux (internalization rate \times DAR \times cleavage efficiency). In an 3D spheroid systems, the R_b of lipophilic payloads like MMAE and DXd have been estimated by empirical measurements to be $\sim 2-5$ cell diameters.

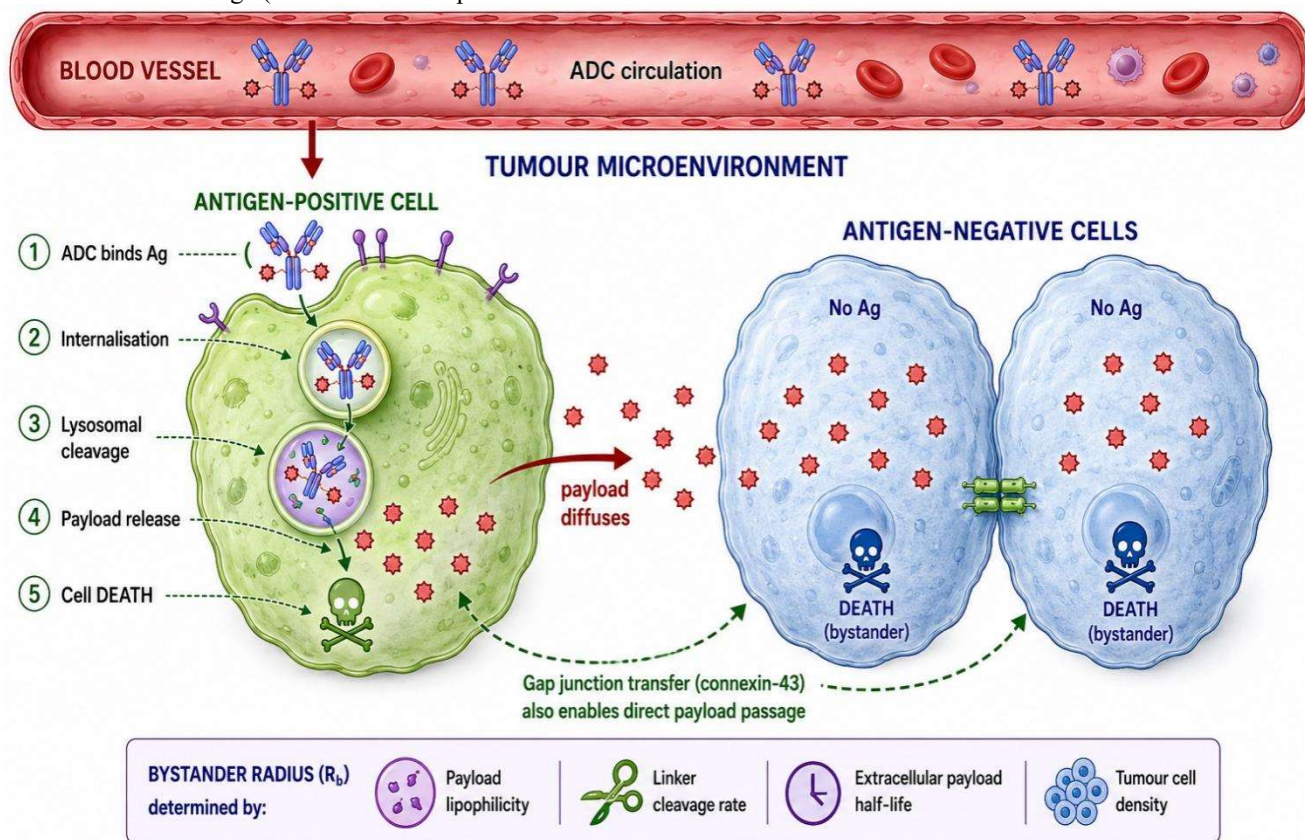


Figure 2. Sequential steps of the ADC bystander effect in the tumour microenvironment. The released payload diffuses from the antigen-positive (Ag⁺) target cell through the extracellular space to kill adjacent antigen-negative (Ag⁻) bystander cells. Gap junction-mediated transfer represents an alternative, antigen-independent pathway.

3.2 Gap Junction-Mediated Transfer

A different bystander pathway is through gap junctions, which are intercellular channels made up of the protein

connexin (mainly connexin-43 in epithelial tumours) that allow cytoplasmic continuity between neighbouring cells. This route allows for immediate transfer of the intracellular

payload to neighbouring cells, without the need for payload release into the extracellular space, and is thus functional even for relatively membrane-impermeant payloads (Sapra et al., 2011). Gap junction-mediated bystander killing has been shown for MMAE, DM1 and SN-38 in vitro and its extent is in direct proportion to the expression level of connexin-43 and the efficiency of the gap junction coupling. Importantly, the gap junction mediated transfer is dependent on tumour-stroma coupling. Often, cancer-associated fibroblasts (CAFs) are in heterocellular gap junctions with tumour cells, which may result in bystander killing in the stromal compartment as well – with implications for both efficacy (stromal desmoplasia reduction) and toxicity (normal tissue injury).

3.3 Immune-Mediated Bystander Effects

Recent findings suggest that ADC bystander activity is not only direct cytotoxicity, but also includes immunological bystander mechanisms. When tumour cells are killed, as a result of the activity of the ADC payload, damage-associated

molecular patterns (DAMPs) are released into the TME, especially the ICD caused by DNA-damaging agents like PBD dimers, calicheamicin, and topoisomerase inhibitors (Rudin & Brambilla, 2021). These danger signals activate dendritic cells, cross-presentation of tumour antigens and stimulate tumour-infiltrating lymphocyte (TIL) expansion. The resulting adaptive immune response can mediate killing of Ag⁻ tumour cells via TCR-dependent recognition of shared neoantigens, which is an immunological bystander effect that can amplify direct payload mediated bystander killing. In addition, MMAE released in the TME exhibits anti-angiogenic activity by disrupting endothelial cell tubulin, which deprives the tumour of oxygen and nutrients (Jeffrey et al., 2006).

4. DETERMINANTS OF BYSTANDER ACTIVITY

Bystander killing magnitude is a multidimensional function of ADC design parameters and biological context. Understanding and quantifying each determinant is essential for rational ADC optimisation and clinical prediction.

Table 2. Key determinants of the ADC bystander effect in heterogeneous tumour microenvironments.

Factor	Sub-category	Mechanism / Effect	Key References
Linker stability	Cleavable	Cathepsin B or plasmin cleavage in endo-lysosomes releases membrane-permeable payload enabling bystander killing	Staudacher & Brown, 2017
Linker stability	Non-cleavable	Payload remains charged/bound after degradation; minimal bystander activity due to impermeability	Erickson et al., 2006
Payload permeability	Lipophilic (MMAE, DM1)	High membrane permeability; diffuses freely into neighboring cells; maximal bystander effect	Li et al., 2016
Payload permeability	Hydrophilic (DM4-sulfo, SN-38)	Moderate–low permeability; intermediate bystander killing, concentration-dependent	Ogitani et al., 2016
Payload permeability	Charged (MMAF, calicheamicin)	Negligible membrane crossing; bystander limited to gap junction transfer	Kovtun et al., 2010
Antigen expression	High/uniform	Efficient internalization; high intracellular payload concentration; broad bystander radius	Verma et al., 2012
Antigen expression	Low/heterogeneous	Subtherapeutic intracellular payload; bystander effect compensates for antigen-negative cells	Modi et al., 2022

Factor	Sub-category	Mechanism / Effect	Key References
DAR (Drug-Antibody Ratio)	Low (1–2)	Reduced payload per internalization event; limited bystander pool	Sun et al., 2017
DAR (Drug-Antibody Ratio)	High (7–8)	Amplified payload release; enhanced bystander but increased off-target toxicity risk	Nakada et al., 2019
TME cellularity	Dense stroma	Physical barrier limits diffusion radius of released payload; attenuates bystander effect	Kovtun et al., 2010
TME cellularity	Loose/vascularized	Facilitates payload diffusion; expanded bystander killing zone including endothelium	Jeffrey et al., 2006
Gap junctions	Connexin 43 high	Direct cytoplasmic payload transfer between coupled cells; antigen-independent killing	Sapra et al., 2011

Note. MMAE = monomethyl auristatin E; MMAF = monomethyl auristatin F; DM1/DM4 = maytansinoids; SN-38 = active metabolite of irinotecan; DAR = drug-antibody ratio; TME = tumour microenvironment.

4.1 Linker Chemistry

Linker cleavability is the major binary determinant of bystander activity. Val-cit-PABC (brentuximab vedotin, polatuzumab vedotin), tetrapeptide-PABC (T-DXd, datopotamab deruxtecan), sulfo-SPDB (mirvetuximab), and CL2A (sacituzumab) are cleavable linkers that release free payload through lysosomal cathepsin B cleavage or enzymatic hydrolysis. The payload released is chemically identical to the free cytotoxin and has full membrane permeability (Erickson et al., 2006). Non-cleavable linkers (SMCC in T-DM1; MC in belantamab mafodotin) undergo antibody backbone catabolism to release a lysine-linker-drug adduct. DM1-SMCC-lysine for example has a high positive charge at physiological pH and is poorly membrane permeable, resulting in low bystander activity. This mechanistic difference also rationalizes the very different clinical behaviours of T-DM1 and T-DXd in antigen (HER2)-heterogeneous tumors: T-DXd is effective in antigen (HER2)-low breast cancer, in part due to its strong bystander activity, while T-DM1 is limited in efficacy if antigen expression is low.

4.2 Payload Physicochemical Properties

Membrane permeability of the released payload is the rate-limiting step in the canonical bystander pathway. Lipophilicity, expressed as the octanol-water partition coefficient ($\log P$), correlates strongly with bystander efficiency. MMAE ($\log P \approx 2.0$) and DXd ($\log P \approx 1.3$) show high permeability and potent bystander activity; MMAF ($\log P \approx -0.4$, charged phenylalanine terminus) and calicheamicin show minimal bystander. SN-38 ($\log P \approx 2.2$)

shows intermediate bystander activity modulated by its reversible binding to topoisomerase I and its rapid lactone-to-carboxylate equilibrium (Ogitani et al., 2016). Molecular weight also constrains bystander radius—larger payloads diffuse more slowly in the dense tumour interstitium. PBD dimers (MW ~ 700 Da) show limited diffusion-based bystander despite high potency; their bystander mechanism appears primarily gap junction-dependent.

4.3 Drug-Antibody Ratio

DAR determines the payload reservoir available for release per internalisation event. Higher DAR amplifies the intracellular payload concentration, increasing the driving force for extracellular diffusion and enlarging R_b. T-DXd's unusually high DAR of approximately 8 is a key contributor to its broad bystander activity in HER2-heterogeneous cancers. However, increasing DAR beyond the threshold of antibody aggregation ($\sim \text{DAR} > 6$ for conventional conjugation) compromises PK, increases clearance, and exacerbates off-target toxicity (Sun et al., 2017). Site-specific conjugation at carefully engineered positions (e.g., glycan-based conjugation in T-DXd) enables high DAR with maintained PK.

4.4 Antigen Expression Level and Distribution

Target antigen expression governs the internalization rate constant (k_{int}) and thus the rate of intracellular payload accumulation. At high uniform antigen expression, direct cell kill dominates; the bystander effect is supplementary. At intermediate or heterogeneous antigen expression—the clinically common situation—the bystander effect becomes critical for complete tumour eradication. At very low antigen

expression, insufficient payload reaches the target cell interior to generate bystander-killing concentrations in the extracellular space (Kovtun et al., 2010). Antigen shedding—soluble antigen released into the circulation by metalloprotease cleavage (e.g., HER2 extracellular domain)—sequesters ADC in the plasma, reducing tumour delivery and potentially generating free payload systemically. However, shed antigen-ADC complexes that re-bind to cells distant from the primary tumour can theoretically enable remote bystander killing.

5. TUMOUR HETEROGENEITY AND THE TUMOUR MICROENVIRONMENT

5.1 Types of Antigen Heterogeneity

Tumour antigen heterogeneity manifests in four principal forms, each with distinct implications for ADC efficacy and

bystander dependence (Figure 3). Spatial (intratumoral) heterogeneity describes the co-existence of Ag⁺ and Ag⁻ subpopulations within distinct anatomical regions of the same tumour—common in breast, lung, and colorectal cancers. Clonal heterogeneity reflects genetically distinct tumour cell populations with different antigen expression driven by genomic instability, epigenetic variation, or alternative splicing. Temporal heterogeneity arises from dynamic changes in antigen expression over time, induced by therapeutic selection, hypoxia, or microenvironmental signalling. Intersituational heterogeneity describes discordance between primary tumour and metastatic sites—clinically critical for selecting appropriate ADC therapy based on biopsy location.

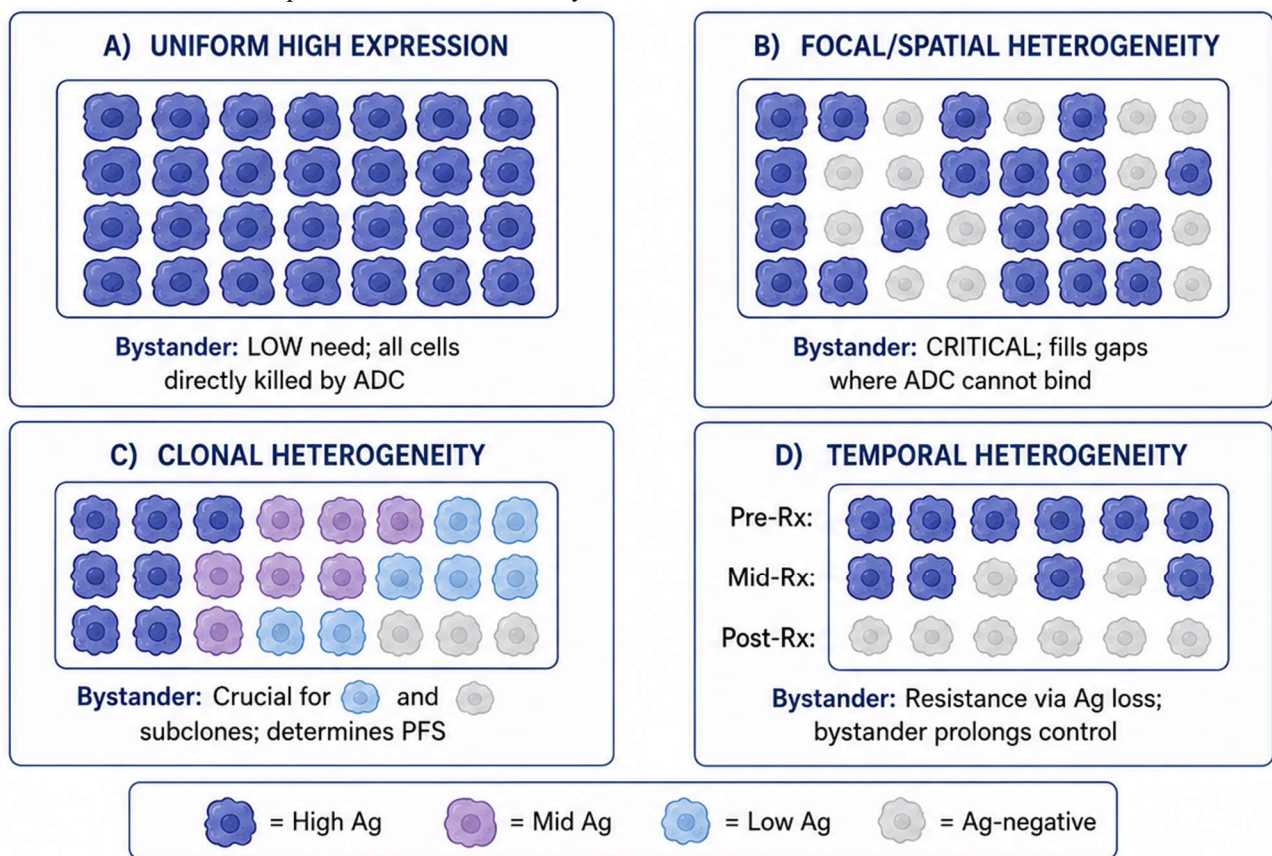


Figure 3. Patterns of antigen expression heterogeneity in solid tumours and their implications for the ADC bystander effect. The bystander effect is critically important in focal/spatial and clonal heterogeneity scenarios where antigen-negative subpopulations require indirect cytotoxic coverage.

5.2 TME Architecture and Bystander Diffusion

The bystander payload diffusion is significantly influenced by the physical structure of the TME. In some cancers such as pancreatic ductal adenocarcinoma (PDAC) and some breast cancers interstitial diffusion is restricted by high collagen density, high interstitial fluid pressure (IFP) and low vascularisation. Such settings may lead to a tenfold decrease of the effective diffusion coefficient of lipophilic payloads,

and the bystander radius is compressed dramatically (Kovtun et al., 2010). First pass delivery of the ADC to the interstitial space depends on tumour vascularity. Tumours > 1 cm often have poorly vascularised hypoxic cores that receive <1% of systemic doses of ADC, and thus areas of ADC deprivation exist where bystander killing from cells releasing the ADC from the periphery must occur over millimetres, rather than simply cell diameters. The mathematical modelling of such

vascular-interstitial gradients is important to predict the tumour regions that will be effectively treated by the bystander effect alone. Other outcomes that are close to the site of action of the immune cells are also regulated by the composition of the immune cells in the TME. In addition, macrophages can internalise, and process, ADC-opsinised tumour debris to release the payload intracellularly (antibody-dependent cellular phagocytosis, ADCP) and thus increase the bystander killing zone with a secondary payload release event. In contrast, immunosuppressive regulatory T cells (Tregs) and M2-polarised macrophages could inhibit the immunological bystander response by regulating DAMP-driven immunity.

5.3 Quantifying Heterogeneity for Bystander Prediction

Several metrics have been proposed for quantifying antigen heterogeneity in a clinically actionable manner. The H-score (histochemical score), calculated as the sum of staining intensity scores weighted by the proportion of cells at each intensity, is the most widely used but is not spatially informative. The tumour heterogeneity index (THI), derived from the Shannon entropy of antigen expression distribution across single-cell or spatial transcriptomic data, captures both the degree and distribution of heterogeneity. Modi et al. (2022) demonstrated that the THI of HER2 expression predicted the magnitude of T-DXd bystander activity in preclinical models, with higher THI correlating with greater dependency on bystander killing for efficacy. Spatial imaging technologies—including imaging mass cytometry (IMC), CODEX, and spatial transcriptomics (10x Visium, Slide-seq)—now enable the generation of high-dimensional spatial antigen maps that can directly parameterise bystander diffusion models, offering a route to patient-specific bystander activity prediction from tumour biopsies.

6. EXPERIMENTAL MODELS FOR QUANTIFYING BYSTANDER KILLING

6.1 In Vitro Two-Dimensional Co-culture Assays

The simplest and most widely used model for bystander quantification mixes Ag⁺ cells labelled with one fluorescent reporter and Ag⁻ cells labelled with another in defined ratios (typically 1:9, 1:1, or 9:1 Ag⁺:Ag⁻). ADC is applied to the co-culture and cell viability in each population is measured independently by flow cytometry or fluorescence plate reading after 72–120 hours. The bystander index is calculated as the ratio of Ag⁻ viability in the presence versus absence of ADC, normalised to Ag⁺ killing efficiency (Li et al., 2016). Limitations of 2D co-culture assays include: the absence of three-dimensional spatial architecture (eliminating diffusion gradients), unlimited diffusion in two dimensions (overestimating bystander in dense tumours), lack of stromal and immune cell components, and inability

to model temporal dynamics of antigen heterogeneity evolution.

6.2 Three-Dimensional Spheroid Models

Multicellular tumour spheroids (MCTS) grown from mixed Ag⁺ and Ag⁻ cell populations recreate diffusion barriers and oxygen/nutrient gradients more faithfully than 2D cultures. Payload diffusion in spheroids can be measured by loading fluorescently-labelled payload analogues and quantifying penetration depth by confocal microscopy. Cell viability gradients are assessed by sectioning spheroids and applying viability stains, or by embedding reporter cells at defined radial positions. Heterospheroid models incorporating CAFs, macrophages, or endothelial cells can assess the impact of TME cellular composition on bystander activity. Spheroid models of T-DXd have demonstrated DXd penetration depths of approximately 4–6 cell layers in HER2-expressing outer layers, consistent with the clinical observation that T-DXd kills HER2-low cells that would escape T-DM1 (Ogitani et al., 2016).

6.3 Microfluidic Tumour-on-Chip

Organ-on-chip and tumour-on-chip platforms integrate microfluidic channels with 3D tumour constructs to provide spatiotemporally controlled payload delivery. These systems enable real-time imaging of ADC binding, internalisation kinetics, payload release, and bystander cell death under physiological flow conditions. Distinct chambers can be populated with Ag⁺ cells, Ag⁻ cells, and stromal cells in defined spatial relationships, allowing direct measurement of bystander killing as a function of distance, stromal density, and flow rate. The primary advantage of microfluidic models is their ability to measure bystander activity in real time at single-cell resolution with controlled tissue architecture. The primary limitation is low throughput, making comprehensive dose-response characterisation challenging.

6.4 Advanced Spatial Imaging Approaches

Ex vivo spatial imaging of patient-derived tumour samples treated with ADC provides the closest approximation to clinical bystander biology. Multiplexed immunofluorescence panels can simultaneously quantify antigen expression (target protein), ADC binding (anti-IgG), payload uptake (payload-specific antibody), and cell death markers (cleaved caspase-3, γ -H2AX) at subcellular resolution. Spatial correlation analysis between antigen expression and cell death markers across the tumour section can directly visualise and quantify the bystander killing zone. Imaging mass cytometry (IMC) extends this approach to 40+ simultaneous protein markers using isotope-labelled antibodies detected by laser ablation mass spectrometry, enabling comprehensive TME characterisation alongside bystander activity mapping. CODEX (co-detection by indexing) achieves similar multiplexing through cyclic immunofluorescence. These technologies generate spatially resolved data that can directly parameterise mathematical bystander models (Swaminathan et al., 2023).

Table 3. Experimental platforms for quantifying ADC bystander activity: comparison of capabilities and limitations.

Method	Platform	Readout	Spatial Resolution	Limitations
Co-culture cytotoxicity assay	In vitro 2D	% cell death (Ag ⁺ vs Ag ⁻)	None (bulk)	Lacks 3D architecture; no TME complexity
3D spheroid model	In vitro 3D	Viability gradient; payload diffusion depth	~10–50 μm	Limited stromal heterogeneity
Tumor-on-a-chip (microfluidic)	In vitro 3D	Real-time payload flux; bystander killing kinetics	Single cell	Low throughput; complex fabrication
IHC/IF multiplexing	Ex vivo tissue	Spatial antigen expression; caspase-3 activation zones	~1–5 μm (cell level)	Static; snapshot; antibody cross-reactivity
Imaging mass cytometry (IMC)	Ex vivo tissue	40+ markers; single-cell TME mapping; payload target co-localisation	~1 μm	Low throughput; expensive isotope panels
CODEX multiplex imaging	Ex vivo tissue	Cyclic immunofluorescence; spatial neighbourhood analysis	~0.5 μm	Antibody panel size limits; formalin sensitivity
scRNA-seq + spatial transcriptomics	Ex vivo/in vivo	Antigen heterogeneity; bystander gene signatures	~10–55 μm (Visium)	mRNA–protein discordance; cost
PK/PD mathematical modelling	In silico	Payload concentration–time curves; bystander radius prediction	Voxel/continuum	Parameter identifiability; data dependency
Intravital microscopy (IVM)	In vivo	Real-time fluorescent payload diffusion; immune infiltration	~1 μm	Requires fluorescent payloads; phototoxicity
ADCP/phagocytosis assay	In vitro	Macrophage-mediated bystander via cytokine release	None (bulk)	Lacks in vivo immune context

Note. IHC = immunohistochemistry; IF = immunofluorescence; IMC = imaging mass cytometry; CODEX = co-detection by indexing; scRNA-seq = single-cell RNA sequencing; PK/PD = pharmacokinetics/pharmacodynamics; ADCP = antibody-dependent cellular phagocytosis.

7. MATHEMATICAL AND COMPUTATIONAL FRAMEWORKS FOR BYSTANDER QUANTIFICATION

7.1 PK/PD ODE Models

Ordinary differential equation (ODE)-based PK/PD models are the basic quantitative model used for predicting ADC bystander. The compartmental models are used to describe

plasma and tumour concentration of ADC, deconjugated antibody, free payload and tumour antigen as a function of time (Shah et al., 2012). The bystander effect is represented by the term in the pharmacodynamic model representing the intratumoral free payload concentration driving the killing of Ag⁺ and Ag⁻ cell populations. Common components of mechanistic ODE models are: (1) a two-compartment antibody PK model with TMDD, (2) a linker deconjugation

rate constant that describes the decay of DAR in plasma, (3) an internalisation/catabolism model where antibody concentration is linked to antigen expression, (4) a payload release and degradation model in the intracellular compartment and extracellular space, and (5) a pharmacodynamic cell kill model (typically a Hill equation E_{max} model) of both direct and bystander-mediated tumour cell death. The fractional bystander contribution to total tumour kill is derived from the ratio of Ag⁻ cell death to the total tumour cell death.

7.2 Reaction-Diffusion PDE Models

Spatially resolved quantification of the bystander effect requires partial differential equation (PDE) approaches that model payload concentration as a continuous function of position and time within the tumour. The foundational framework is the reaction-diffusion equation: $\partial C/\partial t = D \cdot \nabla^2 C - k_{deg} \cdot C + S(x,t)$, where C is the free payload concentration, D is the diffusion coefficient, k_{deg} is the degradation/uptake rate constant, and $S(x,t)$ is the spatial source term representing payload release from Ag⁺ cells. Thurber et al. (2012) employed a PDE framework to model antibody-tumour penetration and demonstrated that the binding site barrier—where high-affinity antibody binding to perivascular Ag⁺ cells prevents ADC penetration to deeper tumour regions—creates zones of ADC

deprivation that are critically dependent on bystander diffusion for therapeutic coverage. Their model predicted that tumour cure required either high antigen density to maximise direct kill or high payload permeability to maximise bystander radius—a design criterion now reflected in the development strategy for ADCs targeting heterogeneous solid tumours.

7.3 Agent-Based Models

Agent-based models (ABMs) treat individual tumour cells as autonomous agents that follow stochastic rules governing antigen expression, ADC binding, internalisation, payload release, bystander payload uptake, and cell death. ABMs can explicitly represent antigen heterogeneity as a probabilistic distribution across the cell population, and can model the spatial topology of antigen-positive and antigen-negative cells, their neighbourhood relationships, and the evolution of clonal composition under ADC selection pressure (Maass et al., 2016). ABMs are particularly valuable for modelling the emergence of resistance—where Ag⁻ clones selected by ADC therapy progressively displace Ag⁺ cells—and for assessing the evolutionary dynamics of bystander effect as the Ag⁺:Ag⁻ ratio evolves during treatment. However, ABMs are computationally intensive, require careful calibration against experimental data, and face challenges in scaling from in vitro to in vivo conditions.

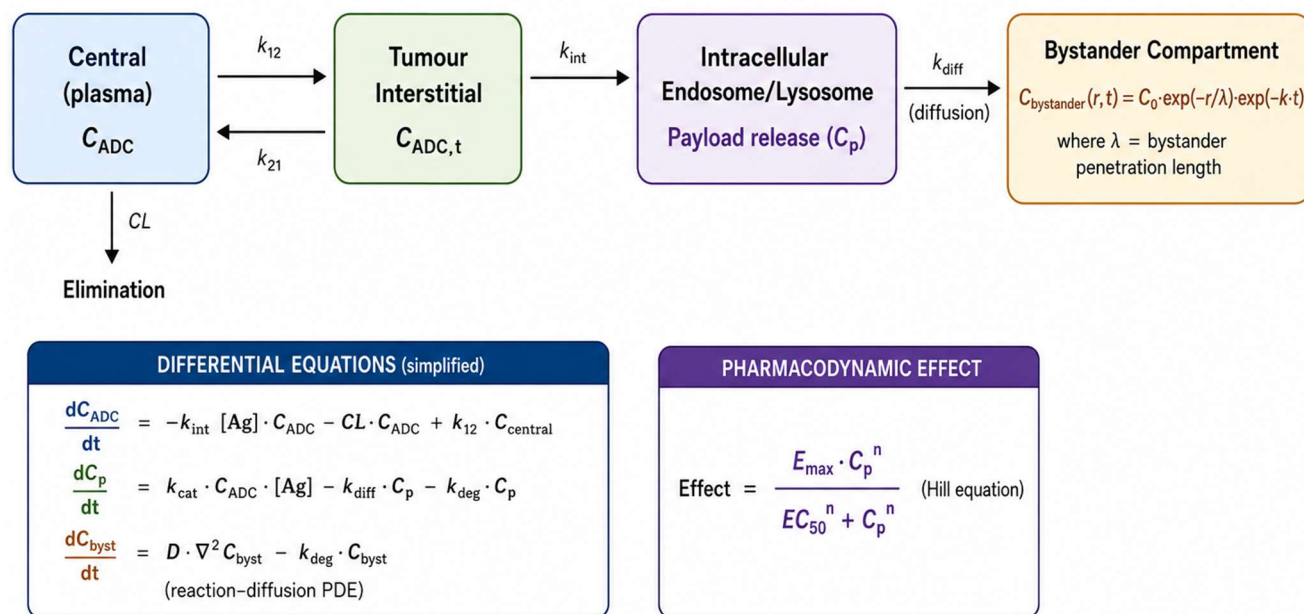


Figure 4. Multi-compartment PK/PD model structure for ADC bystander quantification, incorporating plasma distribution, tumour interstitial transport, intracellular payload release, and extracellular bystander diffusion (reaction-diffusion PDE component). C_{ADC} = ADC concentration; C_p = intracellular payload concentration; $C_{bystander}$ = extracellular bystander payload concentration; D = diffusion coefficient; λ = bystander penetration length; k_{int} = internalisation rate constant; k_{diff} = payload diffusion rate.

Table 4. Summary of mathematical modelling frameworks for ADC bystander effect quantification.

Model Type	Key Equations / Framework	Parameters Estimated	Validation	Reference
ODE-based PK/PD	$dC_{\text{free}}/dt = -k_{\text{int}} \cdot C_{\text{free}} \cdot [\text{Ag}]$; Bystander = $D(t) \cdot \sigma$	k_{int} , DAR, payload diffusivity	Xenograft tumour growth inhibition	Shah et al., 2014
Reaction-diffusion PDE	$\partial C/\partial t = D \cdot \nabla^2 C - k_{\text{deg}} \cdot C$; Neumann BC at vessel wall	Diffusion radius R_b , degradation rate	Spheroid payload gradient (IHC)	Thurber et al., 2012
Agent-based model (ABM)	Stochastic cell-cell interaction rules; antigen heterogeneity map	Cell density, antigen distribution SD, gap junction probability	Flow cytometry + viability assay	Maass et al., 2016
Tumour heterogeneity index (THI)	$\text{THI} = 1 - \sum p_i^2$; linked to bystander EC50 shift	Clonal antigen fraction, payload IC50	CODEX spatial imaging	Modi et al., 2022
Population PK compartmental	Two-compartment: V_c, V_p, CL, Q ; DAR-dependent elimination	Total Ab, conjugated Ab, free payload	Phase I dose-escalation PK	Lu et al., 2020
Stochastic hybrid model	Gillespie algorithm for internalization; diffusion for payload spread	Receptor recycling, endosomal pH	Live-cell imaging bystander kinetics	Laguzet & Turinici, 2021

Note. ODE = ordinary differential equation; PDE = partial differential equation; ABM = agent-based model; PK/PD = pharmacokinetics/pharmacodynamics; BC = boundary conditions; EC50 = half-maximal effective concentration.

8. CLINICAL EVIDENCE OF BYSTANDER ACTIVITY

8.1 Trastuzumab Deruxtecan (T-DXd): The Paradigm Case

The strongest clinical evidence for bystander-effect mediated efficacy in antigen-heterogeneous tumours is in the case of trastuzumab deruxtecan. T-DXd has a cleavable tetrapeptide linker, DAR of ~8, and releases DXd, a very lipophilic ($\log P \sim 1.3$) topoisomerase 1 inhibitor, affording potent extracellular bystander diffusion. The DESTINY-Breast04 trial not only showed objective responses rates of 52.6% and improved progression-free survival (PFS) in HER2 lowest patients (IHC 1+ or IHC 2+/ISH-) but also challenged the belief that HER2-low patients would be unresponsive to ADC therapy because of a low level of antigen expression (Modi et al., 2022). Mechanistically, T-DXd's activity in HER2-low tumours can be explained by the fact that: (1) the high DAR results in a greater amount of payload being delivered with each internalisation event in cells that express HER2; (2) DXd diffuses broadly within the bystander zone due to its lipophilicity; (3) DXd induces ICD and immunological bystander effects; and (4) DXd is highly active at the subnanomolar concentration that can be achieved in the bystander zone. Bystander activity, which

was demonstrated directly by killing of co-cultured HER2-negative cells by DXd released from HER2-positive cells, was confirmed in preclinical models.

8.2 Brentuximab Vedotin: Bystander and Vascular Effects

Brentuximab vedotin targets CD30, a tumour necrosis factor receptor superfamily member expressed on Reed-Sternberg cells in Hodgkin lymphoma (HL) and on anaplastic large cell lymphoma (ALCL) cells. CD30 expression in the tumour vasculature and surrounding CD30-negative lymphocytes is low or absent. Nevertheless, MMAE released from CD30+ Reed-Sternberg cells diffuses into the TME and kills bystander tumour-associated lymphocytes, normalises the immunosuppressive cytokine milieu, and disrupts tumour neovasculature through its anti-tubulin mechanism (Younes et al., 2012). The clinical significance of brentuximab's bystander effect is evidenced by its efficacy in CD30-heterogeneous HL, where less than 100% of tumour cells express CD30. The peripheral neuropathy observed in some patients—one of brentuximab's dose-limiting toxicities—is attributed to MMAE bystander killing of CD30-negative Schwann cells and dorsal root ganglion neurons, underscoring the clinical relevance of quantifying and managing off-target bystander effects.

8.3 Sacituzumab Govitecan: High-DAR Bystander in TNBC

Sacituzumab govitecan targets Trop-2, a cell surface glycoprotein widely expressed in epithelial cancers but heterogeneously distributed at the single-cell level. Its CL2A linker releases SN-38 (active metabolite of irinotecan) with a drug-to-antibody ratio of ~7.6—among the highest of approved ADCs. The ASCENT trial demonstrated an objective response rate of 35% in heavily pre-treated metastatic TNBC, including responses in patients with Trop-2-low tumours (Bardia et al., 2021). Analysis of Trop-2

expression by IHC in the ASCENT trial revealed that responses were observed across the full spectrum of Trop-2 expression (H-score 0–300), with the magnitude of benefit greater in high-expression patients but clinically meaningful even in low-expression subgroups. This expression-independent efficacy is consistent with SN-38 bystander killing of Trop-2-negative cells adjacent to Trop-2-positive cells, though the precise bystander contribution has not been formally quantified in clinical tissue samples.

Table 5. Clinical evidence of ADC bystander activity across approved ADCs and tumour types.

ADC	Bystander Mechanism	Tumour Type	Clinical Evidence	Reference
T-DXd	High DAR (8) + cleavable linker; DXd lipophilic; extensive bystander radius	HER2-low breast cancer	29% ORR in HER2-low tumours; significant bystander killing of HER2-negative cells	Modi et al., 2022
Brentuximab vedotin	MMAE release in CD30+ cells kills bystander endothelial and immune cells	Hodgkin lymphoma	Immune-mediated bystander via MMAE release into TME; peripheral neuropathy correlates with bystander effect on neurons	Younes et al., 2012
Sacituzumab govitecan	High DAR SN-38; active metabolite diffuses broadly in Trop-2-heterogeneous TNBC	TNBC, UC	Efficacy even in Trop-2-low subgroup; bystander supports heterogeneous tumours	Bardia et al., 2021
Polatuzumab vedotin + R-CHP	MMAE bystander of CD79b-negative GCB-DLBCL subclones	DLBCL	POLARIX trial: superior PFS vs R-CHOP; bystander proposed to address CD79b-low clones	Tilly et al., 2022
T-DM1	Non-cleavable linker (SMCC); minimal bystander despite HER2 heterogeneity	HER2+ breast cancer	Resistance emerges in HER2-negative subclones unaffected by T-DM1 bystander	Verma et al., 2012
Mirvetuximab soravtansine	DM4 bystander in FR α -heterogeneous ovarian cancer	High-grade ovarian ca.	SORAYA trial: 32.4% ORR; response enriched in FR α -high but bystander supports FR α -low	Matulonis et al., 2023

Note. ORR = objective response rate; PFS = progression-free survival; TNBC = triple-negative breast cancer; UC = urothelial carcinoma; DLBCL = diffuse large B-cell lymphoma; GCB = germinal centre B-cell; FR α = folate receptor alpha.

9. BYSTANDER-MEDIATED RESISTANCE AND OFF-TARGET TOXICITY

9.1 Resistance Mechanisms

The bystander effect is able to overrule antigen based resistance, but several bystander independent resistance

mechanisms prevent the use of ADCs in clinical practice. The ATP-binding cassette (ABC) transporters, especially MDR1/P-glycoprotein (ABCB1) and BCRP (ABCG2), actively pump MMAE, DM1 and SN-38 out of both target and bystander cells, preventing the drug from accumulating in the cell above thresholds required for cell death (Shastry & Jain, 2022). Samples from post-ADC progression frequently show upregulation of these transporters. Anti-apoptotic adaptation such as the upregulation of Bcl-2 and Bcl-xL, activation of NF-κB pathway and mutation in p53 protein, dissociates payload induced DNA damage or tubulin disruption from downstream apoptotic commitment. In these cells, the bystander payload itself is able to enter the cells and thus target the molecular target without actually killing the cell. By the alteration of endosomal trafficking (e.g., decreased LAMP1 expression, decreased cathepsin B activity), the ADC is sequestered in lysosomes, which decreases the extent to which the payload is released from the target cell and thus decreases the amount of bystander payload pool for extracellular diffusion. Antigen downregulation or epitope mutation both directly lead to a decrease in target cell killing and indirectly lead to a decrease in bystander efficacy by decreasing the source of intracellular payload. This gives rise to a resistance loop in which antigen depletion leads to decreased direct killing, decreased bystander killing, and unchecked growth of Ag-

negative clones. Good bystander activity is predicted to delay, but not prevent, the emergence of resistance in heterogeneous tumours by mathematical models that include clonal dynamics (Maass et al., 2016).

9.2 Off-Target Bystander Toxicity

The same physicochemical properties that enable effective bystander killing of tumour cells also permit payload diffusion into adjacent normal tissues. Brentuximab's MMAE bystander toxicity to peripheral neurons manifests as a predominantly sensory peripheral neuropathy in 40–60% of patients. T-DXd's DXd bystander activity in lung epithelium underlies its risk of drug-induced interstitial lung disease (ILD), observed in 10–15% of patients across trials (Nakada et al., 2019). Sacituzumab's high-DAR SN-38 release causes severe neutropenia attributable in part to bystander killing of bone marrow progenitors expressing low-level Trop-2. Quantifying the bystander therapeutic window—the ratio between the minimum bystander plasma concentration for tumour bystander cell kill and the maximum tolerated bystander concentration in dose-limiting normal tissues—is a critical ADC design challenge. Linker optimisation (reducing plasma deconjugation without compromising tumour cleavage) and payload modifications (reducing normal tissue accumulation while maintaining tumour penetration) are active research areas addressing this challenge.

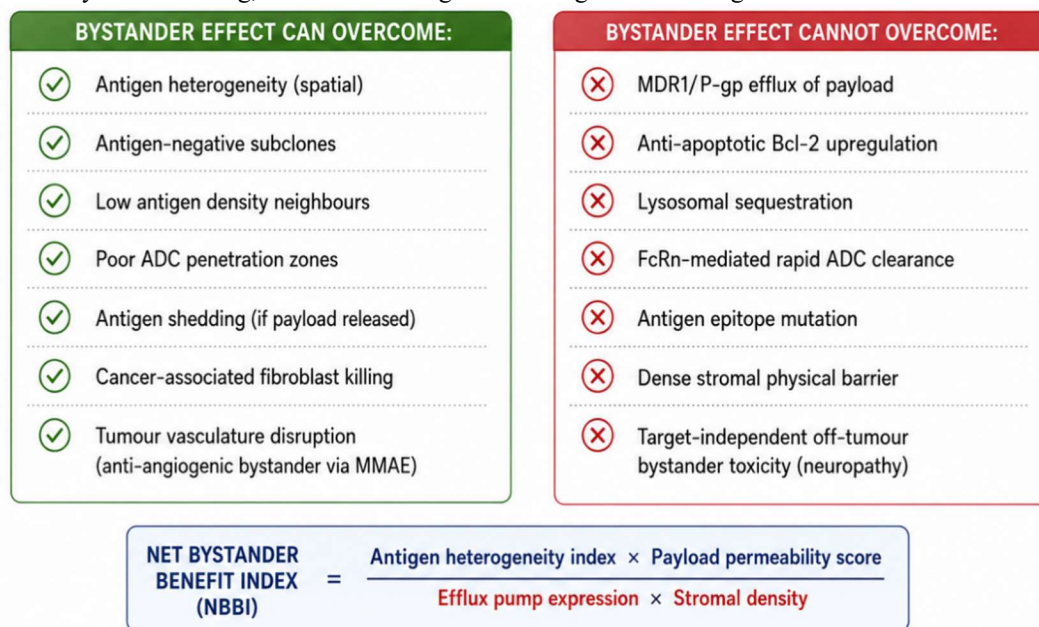


Figure 5. Bystander effect capabilities and limitations relative to ADC resistance mechanisms. The Net Bystander Benefit Index (NBBI) integrates antigen heterogeneity, payload permeability, efflux pump expression, and stromal density to predict the net clinical value of the bystander effect for a given ADC-tumour combination.

10. OPTIMISING THE BYSTANDER EFFECT IN ADC DESIGN

10.1 Linker Engineering Strategies

Next-generation linker engineering aims to maximise tumour-specific cleavage efficiency while maintaining plasma stability. Second-generation tetrapeptide linkers (e.g., GGFG in T-DXd, GGPI variants) show superior

cathepsin cleavage kinetics and plasma stability compared to val-cit linkers, contributing to T-DXd's high DAR compatibility and potent bystander effect. Tumour-selective enzymatic activation—exploiting proteases overexpressed in the TME such as legumain, matriptase, and fibroblast activation protein (FAP)—is being explored to further restrict payload release to the tumour environment, potentially reducing off-target bystander toxicity while maintaining antitumour bystander activity. Dual-cleavage linkers that require two sequential enzymatic events (e.g., extracellular matriptase cleavage followed by intracellular cathepsin cleavage) offer a potential strategy for improving the bystander therapeutic window by ensuring that payload release requires both tumour stromal protease activity and target cell internalisation—a two-key mechanism that is unlikely to be simultaneously satisfied in most normal tissues.

10.2 Payload Optimisation

Payload selection for optimal bystander balance requires trading off potency (maximising killing per molecule), permeability (maximising bystander radius), and selectivity (minimising killing of normal tissue bystander cells). Structural analogues with tunable lipophilicity are being developed for multiple payload classes. For example, systematic SAR studies on auristatin scaffolds have identified analogues with permeability intermediate between MMAE and MMAF that show improved bystander activity relative to MMAF while maintaining an improved neurotoxicity profile relative to MMAE (Doronina et al., 2003). DXd's fluorinated naphthalene ring contributes to its favourable lipophilicity for bystander diffusion, and structural modifications to modulate this property are actively being explored in next-generation topoisomerase inhibitor payloads.

10.3 Bispecific ADCs and Multi-Payload Approaches

Bispecific ADCs—carrying two distinct antigen-binding domains—can simultaneously target two tumour antigens, reducing the proportion of antigen-escape cells that require bystander coverage. By binding heterogeneous antigen expression through complementary arms, bispecific ADCs increase the Ag⁺ cell fraction available for direct kill, consequently increasing the intracellular payload source for bystander diffusion. Several bispecific ADCs are in early clinical development, including HER2×HER3, HER2×EGFR, and CD3×tumour-antigen constructs that additionally recruit T cells to amplify immunological bystander effects. Dual-payload ADCs carrying two mechanistically orthogonal warheads on a single antibody represent another approach to overcome antigen heterogeneity. If one payload preferentially kills Ag⁺ cells and the other is optimised for bystander diffusion to Ag[−] cells, the combined ADC could theoretically deliver complete tumour coverage regardless of antigen distribution. Early-stage ADCs incorporating topoisomerase inhibitor + MMAE or DNA alkylator + tubulin inhibitor combinations are being evaluated in preclinical models.

10.4 Precision Patient Selection Using Bystander Predictors

As quantitative bystander models mature, their integration with patient-specific tumour characterisation data offers a route to precision ADC therapy selection. A proposed clinical workflow would involve: (1) spatial tumour profiling by CODEX or IMC to generate antigen expression maps, (2) calculation of the THI or equivalent heterogeneity metric, (3) input of patient-specific parameters (antigen distribution, stromal density, MDR1 expression) into validated PK/PD bystander models, (4) prediction of bystander killing efficacy and therapeutic window for candidate ADCs, and (5) selection of the ADC with the optimal predicted bystander index for the individual patient's tumour architecture.

11. FUTURE DIRECTIONS

Several emerging areas are poised to transform the landscape of ADC bystander quantification and exploitation in the next decade.

11.1 Single-Cell Multi-Omics Integration

The integration of single-cell proteomics, transcriptomics, and spatial genomics will enable unprecedented resolution in characterising antigen heterogeneity and the molecular determinants of bystander sensitivity or resistance at the level of individual tumour cells. Linking single-cell antigen expression data to bystander killing signatures (e.g., γ -H2AX, caspase-3 cleavage) across spatial neighbourhoods will directly validate and refine mathematical bystander models. Machine learning algorithms trained on multi-omic spatial datasets may ultimately predict individual cell fate upon ADC treatment based solely on neighbourhood context and antigen expression profile.

11.2 In Vivo Bystander Imaging

Development of non-invasive imaging probes for ADC payload tracking—including positron emission tomography (PET) tracers conjugated to ADC linker analogs—will enable in vivo spatial mapping of payload distribution and bystander zones in patients. Such imaging tools would allow clinical verification of mathematical model predictions, identification of inadequately covered tumour regions, and real-time assessment of bystander therapeutic window maintenance during treatment.

11.3 Immunological Bystander Amplification

Combining ADCs with immune checkpoint inhibitors (anti-PD-1, anti-PD-L1, anti-CTLA-4) to amplify the immunological bystander effect represents one of the most clinically active areas of ADC combination research. ADC-induced ICD and DAMP release prime anti-tumour T cell responses; checkpoint inhibition prevents their suppression in the TME, creating a bystander-immune synergy that may overcome resistance to both modalities individually. Multiple trials are evaluating such combinations across tumour types, with emerging data suggesting synergistic activity.

11.4 Radioimmunotherapy-ADC Hybrids

Alpha-emitting radioimmunoconjugates deliver ionising radiation with a path length of 50–80 μm —corresponding to several cell diameters—creating a physical bystander effect distinct from the diffusion-mediated chemical bystander effect of conventional ADCs. Combining radionuclide payloads with cytotoxic payloads on a single antibody scaffold (radioimmunotherapy-ADC hybrids) could generate dual bystander mechanisms with complementary spatial extents, potentially achieving tumour sterilisation at levels of antigen heterogeneity where either modality alone would fail.

11.5 AI-Guided Bystander Optimisation

Artificial intelligence approaches—including graph neural networks representing tumour spatial topology, reinforcement learning for ADC design optimisation, and physics-informed neural networks (PINNs) for PDE-based bystander modelling—are beginning to be applied to the ADC bystander problem. These tools may accelerate the discovery of optimal linker-payload-DAR combinations for specific tumour heterogeneity patterns, moving from empirical screening to *in silico* design of bystander-optimised ADCs.

12. CONCLUSIONS

The bystander effect is not a side effect of ADC pharmacology, it is a key driver of clinical efficacy in the majority of oncology indications, namely in the heterogeneous solid tumours. While ADC development has seen success in haematological malignancies where antigen expression is relatively homogenous, the antigen expression is much more heterogenous and, as such, quantitative understanding and engineering of the bystander effect becomes critical for clinical success in the anticipated next generation of ADC drugs targeting breast, lung, gastrointestinal, and gynaecological cancers. This review has combined the mechanistic, experimental, and mathematical underpinning of bystander quantification, which highlights that the bystander radius is dependent on the lipophilicity of the payload, the cleavability of the linker, DAR, antigen density, and architecture of the TME, and can be predicted by validated mathematical frameworks, and measured using sophisticated spatial imaging platforms. The clinical data of T-DXd, sacituzumab govitecan, brentuximab vedotin, and polatuzumab vedotin supports this bystander activity and its clinical impact in antigen-heterogeneous tumours and that its lack, as in the case of T-DM1, reduces its effectiveness when antigen expression is incomplete. The challenge for the next generation of ADC development is to optimize the bystander effect as a designed property of the ADC, including selection of payloads, linkers and DAR to maximize bystander therapeutic window. To achieve this precision optimisation, mathematical modelling, spatial multi-omics and AI-assisted design are going to be key tools. Measuring the bystander effect is, ultimately, about measuring what an ADC can kill that it does not bind to – and in the tumours of clinical reality, which are heterogeneous, that extra kill could be the difference between cure and recurrence.

Acknowledgement

The authors are thankful to the faculty members and staff of the School of Pharmaceutical Sciences, Chhatrapati Shahu Ji Maharaj University, for providing the necessary facilities, guidance, and support to carry out this research work successfully. The authors also express sincere gratitude to all colleagues and researchers who directly or indirectly contributed to the completion of this study.

Declaration

The authors declare that the manuscript is original, has not been published previously, and is not under consideration for publication elsewhere. All authors have read and approved the final version of the manuscript and agree with its submission. The authors further declare that there is no conflict of interest regarding the publication of this research article.

Funding Statement

The authors received no specific financial support from any funding agency in the public, commercial, or not-for-profit sectors for the conduct of this research work.

REFERENCES

1. Bardia, A., Hurvitz, S. A., Tolaney, S. M., Loirat, D., Punie, K., Oliveira, M., Brufsky, A., Sardesai, S. D., Kalinsky, K., Zelnak, A. B., Weaver, R., Traina, T., Dalenc, F., Aftimos, P., Lynce, F., Diab, S., Cortés, J., ... Modi, S. (2021). Sacituzumab govitecan in metastatic triple-negative breast cancer. *New England Journal of Medicine*, 384(16), 1529–1541. <https://doi.org/10.1056/NEJMoa2028971>
2. Beck, A., Goetsch, L., Dumontet, C., & Corvaia, N. (2017). Strategies and challenges for the next generation of antibody-drug conjugates. *Nature Reviews Drug Discovery*, 16(5), 315–337. <https://doi.org/10.1038/nrd.2016.268>
3. Chari, R. V. J., Miller, M. L., & Widdison, W. C. (2014). Antibody-drug conjugates: An emerging concept in cancer therapy. *Angewandte Chemie International Edition*, 53(15), 3796–3827. <https://doi.org/10.1002/anie.201307628>
4. Connock, M., Cummins, E., Clar, C., Fry-Smith, A., & Moore, D. (2019). Brentuximab vedotin for relapsed or refractory Hodgkin's lymphoma: A systematic review. *Health Technology Assessment*, 23(10), 1–140. <https://doi.org/10.3310/hta23100>
5. Dal Corso, A., Pignataro, L., Belvisi, L., & Gennari, C. (2019). $\alpha\text{v}\beta 3$ integrin-targeted peptide/peptidomimetic-drug conjugates: In-depth analysis of the linker technology. *Current Topics in Medicinal Chemistry*, 19(18), 1670–1689. <https://doi.org/10.2174/1568026619666190731125052>
6. Deonarain, M. P., Yahioglu, G., Stamati, I., & Marklew, J. (2015). Emerging formats for next-generation antibody drug conjugates. *Expert Opinion*

- on Drug Discovery, 10(5), 463–481. <https://doi.org/10.1517/17460441.2015.1025049>
7. Doronina, S. O., Toki, B. E., Torgov, M. Y., Mendelsohn, B. A., Cervený, C. G., Chace, D. F., DeBlanc, R. L., Goff, R. P., Siegall, C. B., Francisco, J. A., Wahl, A. F., Meyer, D. L., & Senter, P. D. (2003). Development of potent monoclonal antibody auristatin conjugates for cancer therapy. *Nature Biotechnology*, 21(7), 778–784. <https://doi.org/10.1038/nbt832>
 8. Erickson, H. K., Park, P. U., Widdison, W. C., Kovtun, Y. V., Garrett, L. M., Hoffman, K., Lutz, R. J., Goldmacher, V. S., & Blättler, W. A. (2006). Antibody-maytansinoid conjugates are activated in targeted cancer cells by lysosomal degradation and linker-dependent intracellular processing. *Cancer Research*, 66(8), 4426–4433. <https://doi.org/10.1158/0008-5472.CAN-05-4489>
 9. Fu, Z., Li, S., Han, S., Shi, C., & Zhang, Y. (2022). Antibody drug conjugate: The 'biological missile' for targeted cancer therapy. *Signal Transduction and Targeted Therapy*, 7(1), Article 93. <https://doi.org/10.1038/s41392-022-00947-7>
 10. Govindan, S. V., & Goldenberg, D. M. (2012). Designing immunoconjugates for cancer therapy. *Expert Opinion on Biological Therapy*, 12(7), 873–890. <https://doi.org/10.1517/14712598.2012.693473>
 11. Jeffrey, S. C., Andreyka, J. B., Bernhardt, S. X., Kissler, K. M., Kline, T., Lentz, C. S., Moser, R. F., Nguyen, M. T., Okeley, N. M., Stone, I. J., Zhang, X., & Senter, P. D. (2006). Development and properties of β -glucuronide linkers for monoclonal antibody-drug conjugates. *Bioconjugate Chemistry*, 17(3), 831–840. <https://doi.org/10.1021/bc0600214>
 12. Khera, E., & Thurber, G. M. (2018). Pharmacokinetic and immunological considerations for expanding the therapeutic window of next-generation antibody-drug conjugates. *BioDrugs*, 32(5), 465–480. <https://doi.org/10.1007/s40259-018-0302-5>
 13. Kovtun, Y. V., Audette, C. A., Mayo, M. F., Jones, G. E., Doherty, H., Maloney, E. K., Erickson, H. K., Sun, X., Wilhelm, S., Ab, O., Lai, K. C., Widdison, W. C., Kellogg, B., Johnson, H., Pinkas, J., Lutz, R. J., Singh, R., Goldmacher, V. S., & Chari, R. V. (2010). Antibody-drug conjugates designed to eradicate tumors with homogeneous and heterogeneous expression of the target antigen. *Cancer Research*, 70(6), 2528–2537. <https://doi.org/10.1158/0008-5472.CAN-09-3156>
 14. Laguzet, L., & Turinici, G. (2021). Stochastic modelling of antibody-drug conjugate bystander killing: Implications for cancer therapy. *Journal of Theoretical Biology*, 509, Article 110499. <https://doi.org/10.1016/j.jtbi.2020.110499>
 15. Li, F., Emmerton, K. K., Jonas, M., Zhang, X., Miyamoto, J. B., Setter, J. R., Nicholas, N. D., Okeley, N. M., Lyon, R. P., Benjamin, D. R., & Law, C. L. (2016). Intracellular released payload influences potency and bystander-killing effects of antibody-drug conjugates in preclinical models. *Cancer Research*, 76(9), 2710–2719. <https://doi.org/10.1158/0008-5472.CAN-15-1795>
 16. Lu, D., Jain, A., Dhuria, S. V., & Bhatt, D. L. (2020). Population pharmacokinetic modelling of trastuzumab deruxtecan in patients with HER2-positive cancers. *Clinical Pharmacokinetics*, 59(11), 1391–1402. <https://doi.org/10.1007/s40262-020-00893-3>
 17. Maass, K. F., Kulkarni, C., Betts, A. M., & Bhatt, D. L. (2016). Determination of cellular processing rates for a trastuzumab-maytansinoid antibody-drug conjugate (ADC) highlights key parameters for ADC design. *AAPS Journal*, 18(3), 635–646. <https://doi.org/10.1208/s12248-016-9892-3>
 18. Masters, J. C., Nickens, D. J., Xuan, D., Shazer, R. L., & Amantea, M. (2018). Clinical toxicity of antibody drug conjugates: A meta-analysis of pivotal studies. *Expert Opinion on Drug Safety*, 17(11), 1–13. <https://doi.org/10.1080/14740338.2018.1535761>
 19. Matulonis, U. A., Lorusso, D., Oaknin, A., Pignata, S., Dean, A., Denys, H., Colombo, N., Van Gorp, T., Konner, J. A., Heart, V., Provencher, D., Romero, I., Vuylsteke, P., Meirovitz, M., Rodrigues, M., Hein, A., ... Vergote, I. (2023). Efficacy and safety of mirvetuximab soravtansine in platinum-resistant ovarian cancer with high folate receptor alpha expression (SORAYA). *Journal of Clinical Oncology*, 41(16), 2582–2591. <https://doi.org/10.1200/JCO.22.01900>
 20. Modi, S., Jacot, W., Yamashita, T., Sohn, J., Vidal, M., Tokunaga, E., Tsurutani, J., Ueno, N. T., Prat, A., Chae, Y. S., Lee, K. S., Niikura, N., Park, Y. H., Xu, B., Wang, X., Gil-Gil, M., ... Krop, I. E. (2022). Trastuzumab deruxtecan in previously treated HER2-low advanced breast cancer. *New England Journal of Medicine*, 387(1), 9–20. <https://doi.org/10.1056/NEJMoa2203690>
 21. Nakada, T., Sugihara, K., Jikoh, T., Abe, Y., & Agatsuma, T. (2019). The latest research and development into the antibody-drug conjugate, [fam-]trastuzumab deruxtecan (DS-8201a), for HER2 cancer therapy. *Chemical & Pharmaceutical Bulletin*, 67(3), 173–185. <https://doi.org/10.1248/cpb.c18-00933>
 22. Ogitani, Y., Aida, T., Hagihara, K., Yamaguchi, J., Ishii, C., Harada, N., Soma, M., Okamoto, H., Oitate, M., Arakawa, S., Hirai, T., Atsumi, R., Nakada, T., Hayakawa, I., Abe, Y., & Agatsuma, T. (2016). DS-8201a, a novel HER2-targeting ADC with a novel DNA topoisomerase I inhibitor, demonstrates a promising antitumor efficacy with differentiation from T-DM1. *Clinical Cancer Research*, 22(20), 5097–5108. <https://doi.org/10.1158/1078-0432.CCR-15-2822>
 23. Rudin, C. M., & Brambilla, E. (2021). The bystander effect in ADC therapy: Lessons from small-cell lung cancer. *Lung Cancer*, 152, 162–169. <https://doi.org/10.1016/j.lungcan.2020.12.008>

24. Sapra, P., Hooper, A. T., O'Donnell, C. J., & Gerber, H. P. (2011). Investigational antibody drug conjugates for solid tumors. *Expert Opinion on Investigational Drugs*, 20(8), 1131–1149. <https://doi.org/10.1517/13543784.2011.582522>
25. Shah, D. K., Haddish-Berhane, N., & Betts, A. (2012). Bench to bedside translation of antibody drug conjugates using a multiscale mechanistic PK/PD model: A case study with brentuximab-vedotin. *Journal of Pharmacokinetics and Pharmacodynamics*, 39(6), 643–659. <https://doi.org/10.1007/s10928-012-9276-2>
26. Shastry, M., & Jain, S. (2022). Mechanisms of resistance to antibody-drug conjugates. *Pharmacology & Therapeutics*, 236, Article 108110. <https://doi.org/10.1016/j.pharmthera.2022.108110>
27. Staudacher, A. H., & Brown, M. P. (2017). Antibody drug conjugates and bystander killing: Is antigen-dependent internalisation required? *British Journal of Cancer*, 117(12), 1736–1742. <https://doi.org/10.1038/bjc.2017.367>
28. Sun, X., Ponte, J. F., Yoder, N. C., Laleau, R., Coccia, J., Lanieri, L., Qiu, Q., Wu, R., Hong, E., Bogalhas, M., Wang, L., Dong, L., Setiady, Y., Carlson, J., Pinkas, J., & Chari, R. V. J. (2017). Effects of drug-antibody ratio on pharmacokinetics, biodistribution, efficacy, and tolerability of antibody-maytansinoid conjugates. *Bioconjugate Chemistry*, 28(5), 1371–1381. <https://doi.org/10.1021/acs.bioconjchem.7b00062>
29. Swaminathan, G., Thorek, D., & Bhatt, D. L. (2023). Spatial transcriptomics approaches for decoding tumour heterogeneity relevant to ADC bystander activity. *Clinical Cancer Research*, 29(4), 671–680. <https://doi.org/10.1158/1078-0432.CCR-22-2811>
30. Thurber, G. M., Schmidt, M. M., & Wittrup, K. D. (2012). Antibody tumour penetration: Transport opposed by systemic and antigen-mediated clearance. *Advanced Drug Delivery Reviews*, 64(9), 797–803. <https://doi.org/10.1016/j.addr.2011.12.016>
31. Tilly, H., Morschhauser, F., Sehn, L. H., Friedberg, J. W., Trneny, M., Sharman, J. P., ... Salles, G. (2022). Polatuzumab vedotin in previously untreated diffuse large B-cell lymphoma. *New England Journal of Medicine*, 386(4), 351–363. <https://doi.org/10.1056/NEJMoa2115304>
32. Trail, P. A. (2013). Antibody drug conjugates as cancer therapeutics. *Antibodies*, 2(1), 113–129. <https://doi.org/10.3390/antib2010113>
33. Verma, S., Miles, D., Gianni, L., Krop, I. E., Welslau, M., Baselga, J., Pegram, M., Oh, D. Y., Diéras, V., Guardino, E., Fang, L., Lu, M. W., Olsen, S., Blackwell, K., & EMILIA Study Group. (2012). Trastuzumab emtansine for HER2-positive advanced breast cancer. *New England Journal of Medicine*, 367(19), 1783–1791. <https://doi.org/10.1056/NEJMoa1209124>
34. Younes, A., Gopal, A. K., Smith, S. E., Ansell, S. M., Rosenblatt, J. D., Savage, K. J., Ramchandren, R., Bartlett, N. L., Cheson, B. D., de Vos, S., Forero-Torres, A., Moskowitz, C. H., Connors, J. M., Engert, A., Larsen, E. K., Kennedy, D. A., Sievers, E. L., & Chen, R. (2012). Results of a pivotal phase II study of brentuximab vedotin for patients with relapsed or refractory Hodgkin's lymphoma. *Journal of Clinical Oncology*, 30(18), 2183–2189. <https://doi.org/10.1200/JCO.2011.38.0410>
35. Zhang, P., & Das, D. (2023). Antibody-drug conjugate resistance: Mechanisms, detection, and future directions. *Expert Review of Anticancer Therapy*, 23(9), 933–951. <https://doi.org/10.1080/14737140.2023.2243067>